JOURNAL OF NANO- AND ELECTRONIC PHYSICS
Vol. **7** No 1, 01034(5pp) (2015)

ЖУРНАЛ НАНО- ТА ЕЛЕКТРОННОЇ ФІЗИКИ
Том **7** № 1, 01034(5cc) (2015)

Structural Engineering of Multilayer TiN / CrN System Obtained by the Vacuum Arc Evaporation

O.V. Sobol'[1,*], A.A. Andreev[2], V.A. Stolbovoy[2], V.F. Gorban'[13], N.V. Pinchuk[1], A.A. Meylekhov[1]

[1] *National Technical University "Kharkiv Polytechnic Institute", 21, Frunze Str., 61002 Kharkiv, Ukraine*
[2] *National Science Center Kharkiv Institute of Physics and Technology, 1, Akademicheskaya Str., 61108 Kharkiv, Ukraine*
[3] *Frantsevich Institute for Problems of Materials Science, 3, Krzhizhanovsky Str., 03680 Kyiv-142, Ukraine*

(Received 21 November 2014; revised manuscript received 12 March 2015; published online 25 March 2015)

By the X-ray diffraction, electron microscopy, and microindentation methods we have investigated the phase composition, structure, substructure and hardness of vacuum arc multilayer coatings of TiN/CrN system obtained in the range of nitrogen pressure of $1 \cdot 10^{-5}$ ... $5 \cdot 10^{-3}$ Torr when applying continuous and pulsed negative bias potential. Formation of two-phase state with a preferred orientation of the crystallite growth was established at high pressure of (1 ... 5)·10^{-3} Torr and feeding of negative DC bias potential: $U_b = -20$ V – texture axis [100], at -230 V – texture axis [111]. Based on the studies of substructural state, connection of the transition to the superhard (57 GPa) state with decrease in the crystallite size and microstrain in TiN layers was established.

Keywords: Vacuum-arc method, Pressure, Bias potential, CrN, TiN, Texture, Substructure, Microstrain, Size of crystallites.

PACS numbers: 81.07.Bc, 61.05.cp, 68.55.jm, 61.82.Rx

1. INTRODUCTION

Study of the regularities of formation of nanolayered TiN/CrN-coatings obtained by vacuum-arc evaporation method is of scientific and practical interest. From the point of view of the practical application, such a coating structure allows to combine high wear resistance of the coating and low wear of the counterbody [1-3]. TiN/CrN-coatings showed high efficiency in the case of their use on cutting tools when cutting hard materials [4].

Scientific interest is connected with deepening understanding of the little-studied processes of formation of nanolayered structures based on mutually soluble systems of the TiN/CrN type in the conditions of deposition of highly ionized excited components of the vacuum-arc plasma streams [5, 6].

Therefore, the aim of the present work was to perform complex investigations on the influence of the key physical and technological parameters on the structural state of multilayer coatings that can be the basis for development of the principles of structural engineering of multilayer nitride coatings.

2. TECHNIQUE FOR PREPARATION AND STUDY OF THE SAMPLES

Multilayer two-phase nanostructured TiN/CrN-coatings were deposited in the vacuum-arc plant "Bulat-6". Titanium VT 1-0, dilute chromium alloy VKh1-17 and active gas – nitrogen (99.95 %) were used as the cathode materials. Coatings were deposited on the surface of the samples of 20 × 20 × 2 mm made of 18N10T steel prepared by standard grinding and polishing methods. The deposition procedure of multilayer coatings consisted of the following stages. Vacuum chamber was evacuated to the pressure of 10^{-5} torr. Then, a negative potential of 1 kV was applied to the rotating device with the substrate-holder, evaporator was switched on and cleaning of the surface of the first of two substrates was carried out by bombardment of chromium ions during 3-5 min. Hereupon, substrate-holder was rotated by 180° and the same cleaning of the second substrate was performed. Then, both evaporators were simultaneously activated, nitrogen was supplied to the chamber and the first CrN layer was deposited on the one side, and TiN layer – from another side.

Deposition process was carried out at the following operating conditions. After deposition of the first layer, both evaporators were switched off, substrate-holder was rotated by 180°, and both evaporators were simultaneously switched on again. Arc current during deposition was 85-90 A, nitrogen pressure (P_N) in the chamber was varied within the range of 10^{-5}-$5 \cdot 10^{-3}$ torr, distance between evaporator and substrate was 250 mm, substrate temperature (T_s) was in the range of 250-350 °C. Coatings of the thickness of about 7 μm were obtained. One pair of two TiN/CrN nanolayers had thickness of about 40 nm, at that thickness of each nanolayer was equal to about 20 nm.

Multilayer nanostructured TiN/CrN-coatings with simultaneous ion implantation during production were deposited when applying to the substrate-holder along with a negative constant potential of a pulsed potential with the pulse duration of 10 μs, repetition frequency of 7 kHz and amplitude to 800 V. The main advantage of this method of plasma-based ion implantation and deposition (PBII&D-method) in the synthesis of two-phase TiN/CrN nanostructures consists in the substantial decrease in the substrate heating up temperature during deposition (below 200 °C) that should block an appreciable diffusion mixing of the system components.

Phase composition, structure and substructural characteristics were investigated by the X-ray diffractometry method (DRON-3M) using Cu-Kα-radiation. Graphite monochromator which was placed in the secondary

* sool@kpi.kharkov.ua

beam (in front of the detector) was used for monochromatization of the detected radiation. Study of the phase composition, structure (texture, substructure) was performed using ordinary techniques of the X-ray diffractometry by analyzing the position, intensity and shape of the diffraction reflexes profiles. Tables of The International Center for Diffraction Data (ICDD) the Powder Diffraction File (PDF) were used to decrypt the diffraction patterns. Substructural characteristics were determined by the approximation method [7].

Microindentation was carried out on the device "Micron-gamma" with a load to $F = 0.5$ N by the diamond Berkovich pyramid with the sharpening angle of 65°, automatically performed load and unload during 30 s.

3. RESULTS AND DISCUSSION

In Fig. 1 we present the micrographs of the fracture of TiN/CrN coatings obtained without (a) and with pulse high-voltage stimulation (b).

It is seen that a cellular structure (Fig. 1) is formed on the surface both in the absence of ion stimulation of the coating growth and with its presence; and structure of the coating fracture shows a columnar shape of the growing grains-crystallites, however, supply of a high-voltage pulse potential leads to a some smoothening of the growing surface (Fig. 1b) due to higher mobility of the deposited in this case film forming particles and to a fibrous growth structure with smaller grain size in the sectional plane of the parallel surface.

According to the X-ray diffractometry data, when applying the constant potential of $U_b = -230$ V without pulse action depending on the pressure in the range of 10^{-4}-$5{\cdot}10^{-3}$ torr, there occurs the change in the structural state from the polycrystalline without preferred orientation to the textured one with the axis [111] perpendicular to the growth surface (the latter is exhibited in a relative increase in the intensity from the peaks of the family of planes {111} – Fig. 2, spectra 3, 4 and also after treatment and selection of the profiles in Fig. 3a, b).

At the relatively low pressure of $1{\cdot}10^{-3}$ torr, the bi-textured state with the axis of preferred orientation [100] and [110] was formed that is associated with a high mobility of the film forming atoms; and at the lowest pressure of $1{\cdot}10^{-4}$ torr – texture with the axis [311]. Appearance of the latter in nitrides of the transition metals with a simple cubic lattice of the NaCl structural type obtained by the vacuum-arc evaporation is associated with the radiation effect of the particles accelerated in the field of the negative bias potential.

Thus, with decreasing pressure, when the mean free path increases and the collision energy loss decreases, there occurs the transition from the strained state texture [111], which is formed at a large content of nitrogen atoms in the lattice [8], and textures [100] and [110] formed at high mobility of the film forming atoms under ion impact at the average pressure, to the texture [311] defined by the radiation effect at the lowest pressure.

Data about the change in the peaks intensity determined by the appearance of the preferred orientation in the pressure range of $(1\text{-}5){\cdot}10^{-3}$ torr for the constituent layers of the TiN and CrN phases are given in Fig. 4.

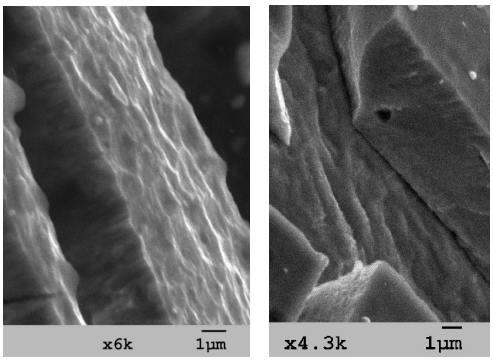

Fig. 1 – Fractographs of the fracture of multilayer TiN/CrN coatings obtained at $U_b = -230$ V, $P_N = 0.005$ torr, $T_s = 250$ °C: without (a) and with (b) pulse stimulation

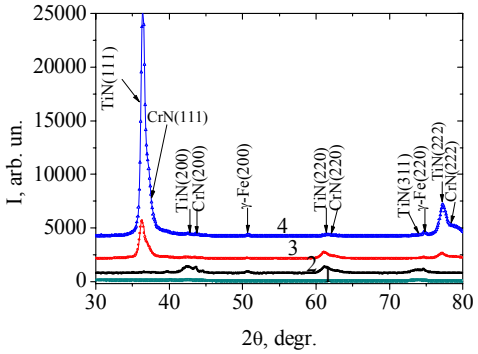

Fig. 2 – Regions of the diffraction spectra of the TiN/CrN coatings obtained at $U_b = -230$ V and P_N, torr: 1 – $1{\cdot}10^{-4}$, 2 – $1{\cdot}10^{-3}$, 3 – $3{\cdot}10^{-3}$, 4 – $5{\cdot}10^{-3}$

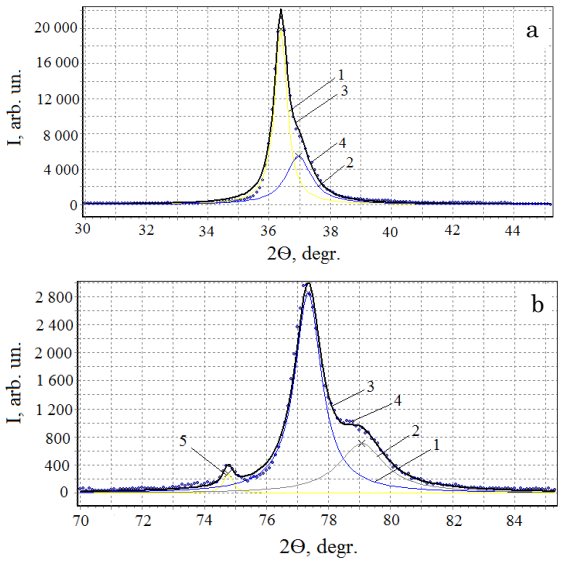

Fig. 3 – Spectral regions with division into components of the diffraction profile of TiN/CrN coating deposited at $U_b = -230$ V and $P_N = 5{\cdot}10^{-3}$ torr: a) 1 – extraction profile of the diffraction curve from the plane (111) of TiN, 2 – extraction profile of the diffraction curve from the plane (111) of CrN, 3 – total approximating curve; 4 – points of the initial data array; b) 1 – extraction profile of the diffraction curve from the plane (222) of TiN, 2 – extraction profile of the diffraction curve from the plane (222) of CrN, 3 – total approximating curve, 4 – points of the initial data array, 5 – extraction profile of the diffraction curve from the plane (311) of TiN

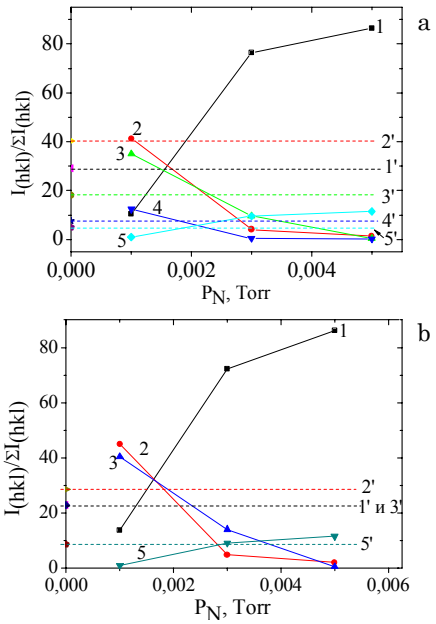

Fig. 4 – Distribution of the diffraction peaks intensities at different deposition pressures for TiN (a) and CrN (b) coatings of TiN/CrN system obtained at $U_b = -230$ V: 1 – (111), 2 – (200), 3 – (220), 4 – (311), 5 – (222), tabulated values (PDF No870629 and PDF No770047): 1' – (111), 2' – (200), 3' – (220), 4' – (311) and 5' – (222)

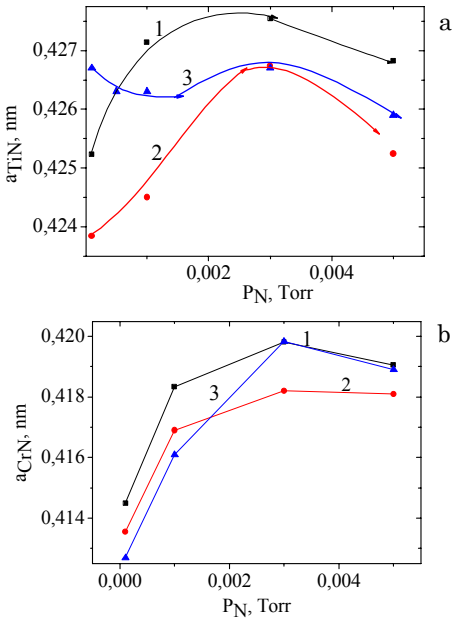

Fig. 5 – Change in the lattice constants of TiN (a) and CrN (b), which are the components of multilayer system, depending on the pressure. 1 – $U_b = -230$ V, $U_{ip} = 0$; 2 – $U_b = -230$ V, $U_{ip} = -700$ V; 3 – $U_b = -20$ V, $U_{ip} = -700$ V

At that, lattice constant for the phases varied synchronously, but not monotonously (Fig. 5). It is seen that with increasing pressure there occurs the growth of the constant along the normal to the surface, and this can be conditioned by both the increase in the nitrogen content in the coating and the increase in the level of compressive stresses. In the case of titanium nitride, increase in the crystal lattice constant to 0.4279 nm can be associated with the fact that CrN phase due to lower thermodynamic stability under the action of ion bombardment and local heating is dissolved in titanium nitride with the formation of (Ti, Cr)N solid solution and increase in the lattice constant. This agrees with the experimental data described in [1], when for thin films of the thickness of 50 nm obtained by sequential deposition of nanolayered TiN/CrN pair with the constant not exceeding 10 nm, by the data of the electron diffraction analysis any two-phase state was not revealed. It follows from the electron diffraction patterns that for this thickness of nanolayers, a cubic phase of (Ti, Cr)N solid solution with NaCl structural type of the crystal lattice was formed during deposition as well as in the case of titanium mononitride.

By the analysis of the obtained dependences, it should be noted a lower value of the lattice constant for both phases during their formation under high voltage pulse action. The reason of this, seemingly, is the decrease in the stress state typical for such action [9].

Supply of high voltage pulses during deposition combined with constant negative potential of – 230 V does not principally change the behavior of the formed phase-structure state of the coatings (Fig. 6).

We can also note the formation of preferred orientation with the axis [111], whose perfectness (at pressures of (3-5)·10^{-3} torr) increases with increasing pressure (see Fig. 4 and Fig. 7).

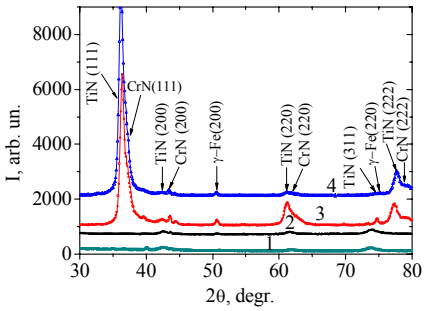

Fig. 6 – Regions of the diffraction spectra of TiN/CrN coatings obtained at $U_b = -230$ V and impulse action $U_{ip} = -700$ V and P_N, torr: 1 – 1·10^{-4}, 2 – 1·10^{-3}, 3 – 3·10^{-3}, 4 – 5·10^{-3}

The principle differences are manifested on the substructural level as significantly smaller crystallites and TiN microstrains of constituent layers at high deposition pressures (Fig. 8a, c). While during the formation of CrN layers, supply of high voltage pulses leads to a higher mean value of the crystallite size at lower microstrain (Fig. 8b, d).

Here we should note that in contrast to titanium nitride, microstrain in chromium nitride increases modes with increasing pressure, however, in the case of pulse action, seemingly, because of the possibility of ordering, such growth is manifested in the least degree.

Decrease in the constant negative bias potential to – 20 V under the pulse high voltage action leads to the qualitative change of the formed structural state that is exhibited on the diffraction spectra (Fig. 9).

It is seen that with increasing pressure, in this case there occurs the formation of another type of preferred orientation of crystallites, namely, with the axis [100] perpendicular to the growth surface plane that is manifested in the increase in a relative peak intensity from the plane (200) in the angular range of $2\theta = 40…45°$ for both TiN and CrN phases (Fig. 10).

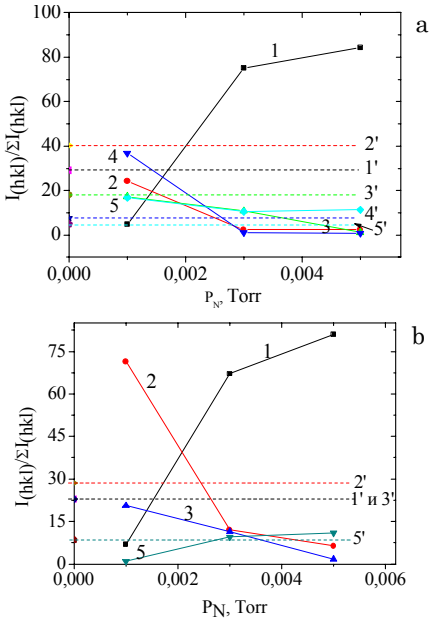

Fig. 7 – Distribution of the diffraction peak intensities at different deposition pressures for TiN (a) and CrN (b) coatings of TiN/CrN system obtained at $U_b = -230$ V and $U_{ip} = -700$ V: 1 – (111), 2 – (200), 3 – (220), 4 – (311), 5 – (222), tabulated values (PDF No870629 and PDF No770047): 1' – (111), 2' – (200), 3' – (220), 4' – (311), 5' – (222)

As seen from the presented in Fig. 11 dependences of the diffraction peak intensity on the nitrogen atmosphere pressure during deposition in the TiN phase, texture with the axis [100] is prevalent starting from the lowest pressures during deposition (Fig. 11a), while in the CrN phase in the medium pressure range one observes formation of the bi-textured state with the axes [100] and [111] (Fig. 11b).

Ratio of titanium nitride-to-chromium nitride volumetric phase content is approximately equal to 1.5 : 1. We should note that in the transition from the lowest pressure during deposition of $1 \cdot 10^{-5}$ torr to a higher one of $1.2 \cdot 10^{-4}$ torr (Fig. 9, spectra 1, 2), phase composition is changed from metal Ti and Cr to titanium nitride with conservation of chromium in the metal state. Formation of chromium nitride of the isomorphic to titanium mononitride modification takes place only at the pressure of $5 \cdot 10^{-4}$ torr (Fig. 9, spectrum 3).

Formation of chromium nitride at higher pressure than of titanium nitride can be explained by the result of primary synthesis of titanium nitride compared with chromium nitride due to higher affinity with nitrogen in Ti-N system than in Cr-N system. Free energy of TiN formation is almost two times more than of CrN [10], and synthesis rate constant is 1.5 times higher.

It is seen from the obtained dependences of the coatings hardness on the deposition pressure presented in Fig. 12 that at a comparatively low constant negative bias potential of – 20 V (Fig. 12, dependence 3) coatings with high hardness are formed at the maximum pressure of $5 \cdot 10^{-3}$ torr. A substantial hardness increment is observed with increasing constant negative potential to – 230 V (Fig. 12, dependences 2 and 3).

Here, pulse action leading to the microstrain decrease and smaller crystallite size in TiN coatings (Fig. 8) conditions a significant increase of the coatings hardness (to 57 GPa).

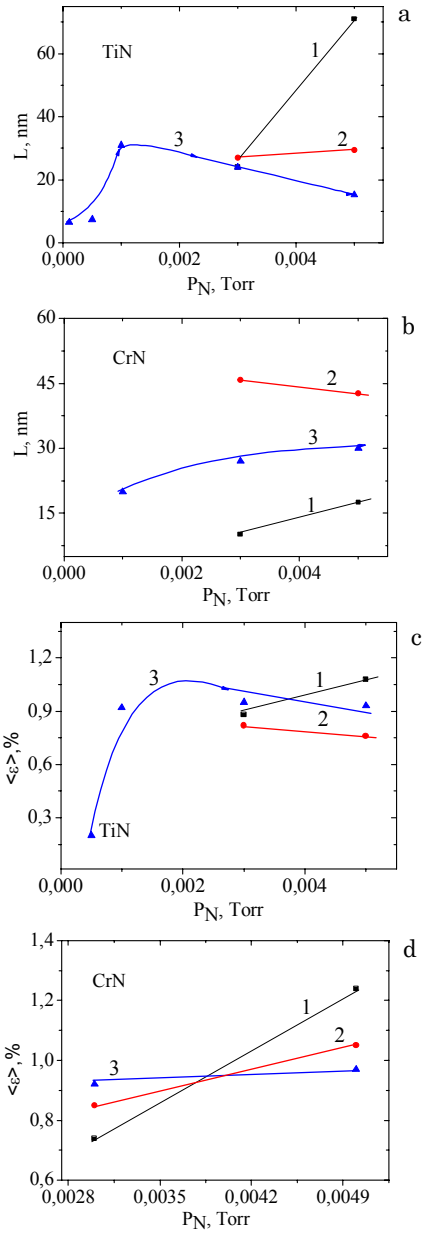

Fig. 8 – Change dependences of the substructural characteristics (average crystallite size, L (a, b) and microstrain, $\langle\varepsilon\rangle$ (c, d)) in crystalline TiN (a, c) and CrN (b, d) phases of multilayer system on the nitrogen atmosphere pressure during deposition P_N: 1 – $U_b = -230$ V, $U_{ip} = 0$; 2 – $U_b = -230$ V, $U_{ip} = -700$ V; 3 – $U_b = -20$ V, $U_{ip} = -700$ V

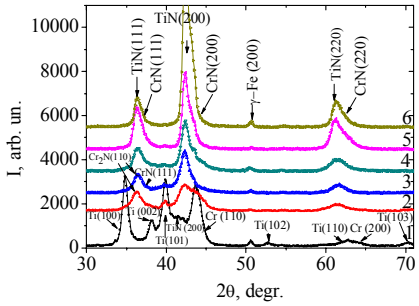

Fig. 9 – Diffraction spectral regions of TiN/CrN coatings obtained at $U_b = -20$ V, impulse action $U_{ip} = -700$ V and P_N, torr: 1 – $1 \cdot 10^{-5}$, 2 – $1.2 \cdot 10^{-4}$, 3 – $5 \cdot 10^{-4}$, 4 – $1 \cdot 10^{-3}$, 5 – $3 \cdot 10^{-3}$, 6 – $5 \cdot 10^{-3}$

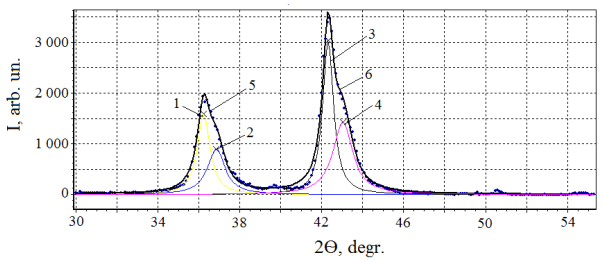

Fig. 10 – Spectral region with division into components of the diffraction profile of TiN/CrN coating deposited at $U_b = -20$ V, $U_{ip} = -700$ V and $P_N = 5 \cdot 10^{-3}$ torr: 1 – extraction profile of the diffraction curve from the plane (111) of TiN, 2 – extraction profile of the diffraction curve from the plane (111) of CrN, 3 – extraction profile of the diffraction curve from the plane (200) of TiN, 4 – extraction profile of the diffraction curve from the plane (200) of CrN, 5 – total approximating curve, 6 – points of the initial data array

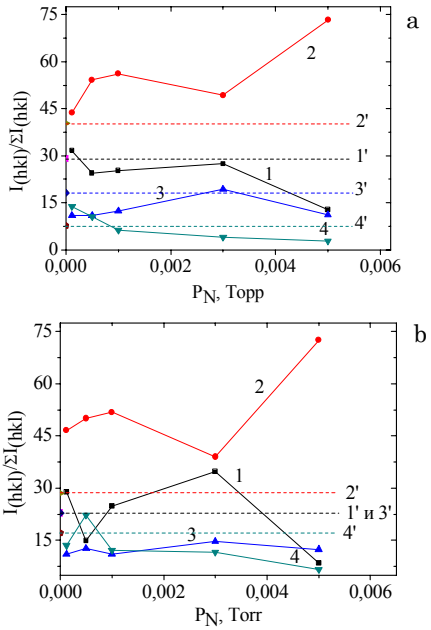

Fig. 11 – Distribution of the diffraction peak intensities at different deposition pressure for TiN (a) and CrN (b) coatings of TiN/CrN system obtained at $U_b = -20$ V and $U_{ip} = -700$ V: 1 – (111), 2 – (200), 3 – (220), 4 – (311), tabulated values (PDF No870629 and PDF No770047): 1' – (111), 2' – (200), 3' – (220) and 4' – (311)

Thus, in the case of coatings deposition in the regime, which combines the constant negative substrate potential (– 230 V) and ion implantation from gas-metal plasma (titanium, chromium and nitrogen) at comparable pressures of nitrogen, a significant hardness increment with respect to the coatings obtained without implantation takes place.

Both the decrease in the average crystallite size in TiN layers and a lower microstrain can be the reason of this increase, as it is seen from the obtained structural results. The latter results imply a higher uniformity in the atom distribution, stimulated pulse implantation of ions accelerated to high energies which possess in this case an increased mobility.

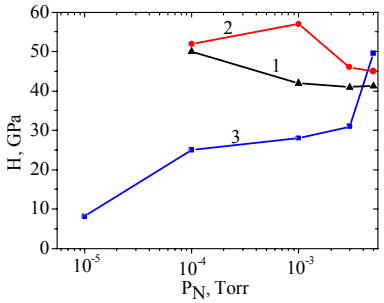

Fig. 12 – Dependence of the microstrain of multilayer TiN/CrN coatings on the nitrogen atmosphere pressure during deposition (P_N): 1 – $U_b = -230$ V, $U_{ip} = 0$; 2 – $U_b = -230$ V, $U_{ip} = -700$ V; 3 – $U_b = -20$ V, $U_{ip} = -700$ V

4. CONCLUSIONS

1. Formation of the two-phase state with more efficient nitride-formation in titanium layers is revealed. Supply of the constant bias potential of – 20 V leads to the appearance of the texture with the axis [100], and when applying higher potential of – 230 V – with the axis [111].

2. Pulse action at – 230 V leads to the appearance of preferred orientation [311] at $P_N = 1 \cdot 10^{-3}$ torr. Texture [111], which, however, is less perfect than in the case of the pulse-free action, is developed at higher pressures.

3. Increase in the pressure of the working nitrogen atmosphere during deposition leads to the lattice constant growth that is associated with saturation of the crystal lattice with nitrogen atoms.

4. Supply of high-voltage pulses due to the increase in the average energy of deposited particles leads to the decrease in the intercrystalline defects and microstrain connected with them.

5. It is established the possibility of obtaining coatings of high hardness to 57 GPa when applying the bias potential of – 230 V and pulse high-voltage action that is connected with the decrease, at that, in the average crystallite size and reduction of the level of intercrystalline microstrain in both TiN and CrN layers.

REFERENCES

1. A.A. Andreyev, L.P. Sablev, S.N. Grigor'yev, *Vakuumno-dugovyye pokrytiya* (Khar'kov: NNTS KhFTI: 2010).
2. Yu.V. Kunchenko, V.V. Kunchenko, I.M. Neklyudov, G.N. Kartmazov, A.A. Andreyev, *Voprosy atomnoy nauki i tekhniki* No 2(90), 203 (2007).
3. M. Oden, J. Almer, G. Hakansson, M. Olsson, *Thin Solid Films* **377-378**, 407 (2000).
4. A.A. Andreev, I.V. Gavrilko, A.G. Gavrilov, A.S. Vereschaka, V.P. Zhed, V.G. Padalka, A.K. Sinelschikov, Pat. № 4 436 830 USA, MKI S04V 35/3. *Coating for metal-cutting tools* (1984).
5. A.D. Pogrebnjak, A.P. Shpak, N.A. Azarenkov, V.M. Beresnev, *Phys.-Usp.* **52** No 1, 29 (2009).
6. Albano Cavaleiro, De Hosson, Th.M. Jeff, *Nanostructured coatings* (Springer: Verlag: 2006).
7. O.V. Sobol', *Phys. Solid State* **53** No 7, 1464 (2011).
8. N.A. Azarenkov, O.V. Sobol, A.D. Pogrebnjak, V.M. Beresnev, S.V. Lytovchenko, O.N. Ivanov, *The materials science of non-equilibrium states of modified surface* (Sumy: Sumy State University: 2012).
9. O.V. Sobol', A.A. Andreev, S.N. Grigoriev, et al., *Metal Sci. Heat Treat.* **54** No 3-4, 195 (2012).
10. G.V. Samsonov, *Nitridy* (Kyiv: Naukova dumka: 1969).